heritage

MDPI

Article

Predicted Dynamic of Biodeterioration in Cultural Heritage Stones Due to Climate Changes in Humid Tropical Regions—A Case Study on the *Rhodotorula* sp. Yeast

Fabio Sitzia [1,2,*], Carla Lisci [1,2], Vera Pires [1,2], Luís Dias [1], José Mirão [1] and Ana Teresa Caldeira [1]

[1] HERCULES Laboratory & IN2PAST, University of Évora, Palácio do Vimioso, Largo Marquês de Marialva 8, 7000-809 Évora, Portugal; clisci@uevora.pt (C.L.); vlcp@uevora.pt (V.P.); luisdias@uevora.pt (L.D.); jmirao@uevora.pt (J.M.); atc@uevora.pt (A.T.C.)

[2] Geosciences Department, School of Sciences and Technology, University of Évora, Rua Romão Ramalho 59, 7000-671 Évora, Portugal

* Correspondence: fsitzia@uevora.pt

Abstract: The recent global warming started at the end of the 19th century, causing an increase in the average temperature of Earth and posing environmental, social, economic, and cultural repercussions. Much tangible cultural heritage is composed of natural stones, which decay due to the combination of chemical, physical, and biological factors. Biodeterioration leads to a loss of the performance requirements and socio-economic value of stone building materials. In the future, the dynamics of biodeterioration will hypothetically vary. This study aims to shed light on this variation by comparing biodeterioration under historical climatic conditions (1995–2014) with a future scenario defined by the IPCC SSP5-8.5 for the reference period 2080–2099. The material tested is Pedra de Ançã (PA), a candidate for World Heritage Stone. Climatic chambers were used to simulate the historical and predicted environmental conditions. The scope of this investigation is to understand the growth dynamic of the biodeteriogen *Rhodotorula* sp. and to study the morphological and aesthetic variations of stone surfaces. Biochemical and micro-topographic analyses highlighted the metabolic activity of the population proliferating under distinct environmental conditions, revealing better adaptability of *Rhodotorula* sp. and higher biocorrosion in the historical climate status with respect to the future.

Keywords: limestone; Pedra de Ançã; global warming; world heritage stone; carbon dioxide; relative humidity; shared socio-economic pathways; building pathology

Citation: Sitzia, F.; Lisci, C.; Pires, V.; Dias, L.; Mirão, J.; Caldeira, A.T. Predicted Dynamic of Biodeterioration in Cultural Heritage Stones Due to Climate Changes in Humid Tropical Regions—A Case Study on the *Rhodotorula* sp. Yeast. *Heritage* **2023**, *6*, 7727–7741. https://doi.org/10.3390/heritage6120406

Academic Editors: Alessandra Bonazza, Lola Kotova and Alessandro Sardella

Received: 12 November 2023
Revised: 30 November 2023
Accepted: 11 December 2023
Published: 15 December 2023

1. Introduction

The base principles of stone chemical–physical weathering under historical [1] and future climatic conditions in the Mediterranean climate area [2] and the subarctic environment [3] have already been investigated from various authors. Research carried out so far on stone biodeterioration mainly concerns historical or actual environmental conditions and their impact on stone decay [4–7]. Understanding biodegradation dynamics, particularly under future climatic conditions distinct from the present, is a topic insufficiently addressed in the literature. Regarding the anticipated shifts in atmospheric CO_2 concentrations due to climate change, some research has shown that exposure to higher than ambient levels of CO_2 can enhance photosynthesis with a fertilizing effect on photosynthesizing stone biodeteriogen organisms (algae, cyanobacteria, and superior plants) [7]. Some superior plants are classified as biodeteriogens, and changes in active tissue quality (wider C/N ratio) and their effects on community dynamics have been discovered [8,9].

However, not all biodeteriogen microbes and plants respond equally to an increase in atmospheric CO_2 [10–12]. Regarding microbes, no differences have been recorded for *Anabaena* sp. [13], *Gloeotrichia natans* [10], *Nannochloropsis gaditana*, and *Nannochloropsis*

maculate [11]. As mentioned above, an overall increase in CO_2 produces an increase in biomass and lipids in microorganisms such as *Chlorella* sp. [14] and cyanobacteria [15].

By contrast, algal and lichen communities do not respond to CO_2 enrichment [16,17]. Regarding superior plant, an overall increase in available CO_2 leads to a stronger response of fast-growing herbaceous species than slower-growing species [8]. Other observations have stabilized a threshold above which plants are CO_2-saturated, and no increases in productivity have been observed [12,18].

In the abovementioned research, stone biodeteriogen communities have been exposed to arbitrary CO_2 concentrations that do not correspond or are outdated from realistic climate change scenarios. This research, instead, proposes the use of up-to-date generation-five scenarios (shared socio-economic pathways, SSPs) formulated by the Intergovernmental Panel on Climate Change (IPCC) in 2021. SSPs indicate that CO_2 global average concentrations by 2100 will range from 393 to 1135 ppm for the lowest (SSP1-1.9) and highest (SSP5-8.5) emission scenarios, respectively [19], contrary to the present-day CO_2 atmospheric concentration, which is around 420 ppm.

A variation in other atmospheric anhydrides such as SO_2 and its effects on stone biodeteriogens are not yet completely understood. Some researchers point out that for some microorganisms, an amount of SO_2 higher than the atmospheric background (commonly $20 < SO_2 < 125$ $\mu g/m^3$) may have a beneficial effect. This has been recorded in certain fungi (e.g., *Penicillium* sp., *Embellicia* sp.) and bacteria (e.g., *Brevibacillus* sp., *Streptoverticillium* sp.) [20]. Additionally, heterotrophic microflora could be the first colonizers of stone materials exposed to a SO_2-bearing atmosphere [21]. When the SO_2 concentration is much higher than the atmospheric background, some biological microorganisms, such as lichens, with rare exceptions, can be negatively affected [22]. In any case, the emissions of SO_2 are going to decline due to policies directed at reducing pollution, especially in urban areas through the disposal of thermic engines in vehicular traffic [23].

Thermo-hygrometric conditions regulate microbial activities, but their modifications due to climate change and its outcomes on biodeteriogen communities are not sufficiently explained. In general, water availability and humidity are the main factors determining biofilm formation, community composition, and, especially, the assortment of species. Some authors have demonstrated that a change in the biomass of phototrophs can happen in response to water availability [24]. Further investigations have found that moisture could be a key factor. Although no direct relationship has been observed, these researchers hypothesized that biofilm distribution may depend on the temporal distribution of moisture and, possibly, transient wetting events [25].

The significance of microorganism colonization on stone surfaces has resulted in a substantial amount of literature examining the mechanisms and rates of the physicochemical degradation of stones in both laboratory and field settings [26–30]. The biological colonization of a stone surface is contingent on intrinsic stone characteristics, such as mineral composition, texture, porosity, and permeability, in addition to the abovementioned environmental factors [26]. The bioreceptivity of limestone extract from phototrophic microorganisms has been linked to effective porosity, capillary and water absorption, water vapor permeability, surface roughness, stone pH, and chemical composition [27]. Another study demonstrated the correlation between the quantification of the surface roughness of stones and the colonization by epilithic organisms, carried out using non-destructive techniques for three distinct types of limestones. It was concluded that a higher surface roughness is linked to enhanced microbial colonization [26].

This paper introduces the biodeterioration dynamics of *Rhodotorula* sp. yeast on limestone by simulating historical (1995–2014) and future climatic conditions (2080–2099) in a humid tropical climate (Figure 1a). *Rhodotorula* sp. is an important and very common pathogen for natural stones, mortars, and paints [31,32].

The choice of tropical climate was essentially made for two reasons:

(i) It affects highly populated areas with considerable building density.

(ii) Thanks to the high average annual temperature and humidity, the tropical humid climates clearly offer ideal conditions for the growth of stone colonizers.

The research questions of this research are the following:

(i) Will climate change favor or reduce the growth of *Rhodotorula* sp. on limestone substrates?
(ii) Given the escalating levels of atmospheric CO_2 and temperatures, is there an anticipated change in the biodegradation caused by *Rhodotorula* sp.?

In this research, the physical biodegradation of the stone surface, usually observed in 2D photography, was evaluated by three-dimensional LIDAR Nano Point Scanner (NPS) modeling [4]. The NPS is an innovative non-contact confocal 3D profile meter measuring altitude in real time, for profile or surface scanning [4]. It is characterized by a measurement range from 0 to 1400 µm. The NPS technique was used to evaluate the interaction between the substrate and the biofilm. Biocolonization affects the rock surface by increasing its roughness. Consequently, this change in topography allows nutrients and water to be simply retained and enhances microbial growth.

The significance of this paper is supported by the annual global financial loss and human diseases due to biological damage to stone building materials and structures [33]. Hence, it is crucial to determine the predicted stone biodegradation, taking into consideration the climate change challenges that urban communities must necessarily face.

Stone Materials Biodeterioration Due to Rhodotorula sp. Yeast

Construction materials, particularly stones, are commonly colonized by microbial populations, whose development is strongly connected with the climatic conditions and the substrate's chemical composition [34]. Among the several types of colonizers, it is generally consensual that eukaryotic strains, including algae, yeasts, and filamentous fungi, represent the most serious threat [35]. Their proliferation and capacity to secrete metabolites may induce both aesthetic and micro-structural alterations by compromising the raw characteristics of stone. Typical examples of metabolites are carotenoids, natural pigments that are part of the class of tetraterpernoid compounds derived from highly unsaturated isoprenes. These bioactive compounds, which may induce yellow, orange, pink, and red hues [36], are mostly produced by filamentous fungi and yeasts, but also bacteria, algae, and lichens [37]. Their main functions are the harvesting of light energy, protection against oxidative damage, and stabilization of certain pigment–protein complexes. *Rhodotorula* sp., through its metabolic activity, is a yeast that produces reddish-pink carotenoids, and its deleterious action has been reported in previous studies [38].

Biodegradation due to *Rhodotorula* sp. is commonly found in indoor environments, affecting a wide variety of lithologies and other construction materials worldwide. Some examples of biofilms are shown in Figure 1b–f where pink spots can be detected on granites, synthetic varnishes, and limestones. The microbial communities found in these environments often consist of other carotene-producing microorganisms, and *Rhodotorula* sp., although it may be present, is not generally the most common and abundant.

In addition to stones, *Rhodotorula* sp. have also been isolated from deep igneous aquifers, 200–400 m below the surface in the Baltic Sea and from deep ice cores of Greenland glaciers at extraordinary depths of 2000 m [38].

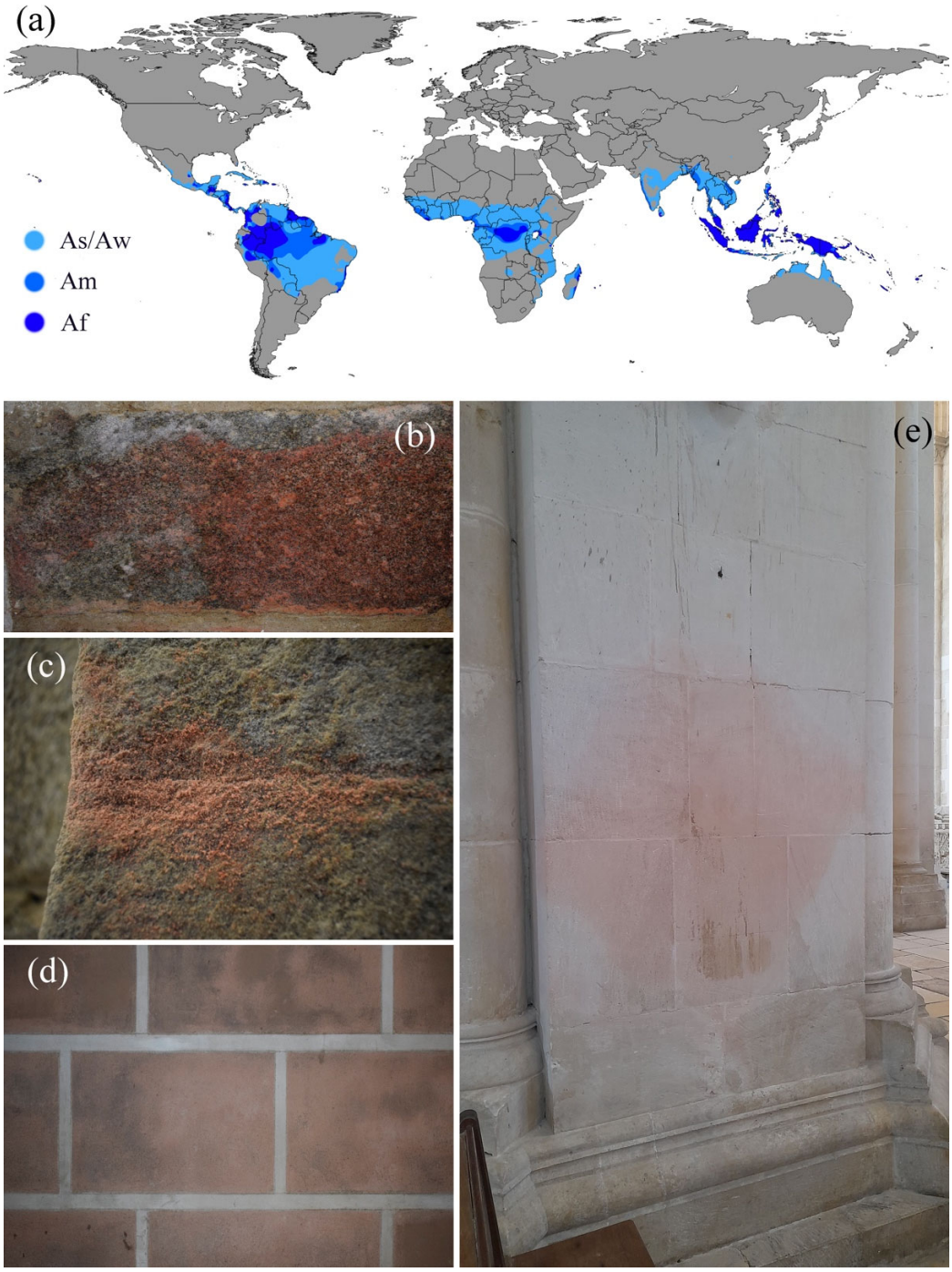

Figure 1. (**a**) Worldwide diffusion of tropical climate [39] (Af = tropical rainforest climate, Am = tropical monsoon climate, As = tropical savanna climate with dry summer, Aw = tropical savanna climate with dry winter); (**b**,**c**) colonization of *Rhodotorula* sp. on granitic substate; (**d**) colonization of *Rhodotorula* sp. on synthetic varnish (Ca–Ti-bearing); (**e**) colonization of *Rhodotorula* sp. on limestone. Photos taken by Fabio Sitzia.

2. Materials and Methods

2.1. Materials

The limestone selected as a substrate for the inoculations is commercially known as *Pedra de Ançã* (*PA*). It is a Portuguese lithotype from Bajocian–Bathonian (Lower Jurassic) geological period [40], mainly used in ancient vernacular architecture as well as other lithotypes of the Mediterranean area [41]. It presents some geological *facies* characterized

by differences in workability, hardness, and porosity [42]. The *facies* utilized in this research is the most porous, soft, and workable. Due to these features, it is suitable for use in various architectural elements. *PA* limestone has been used since the occupation of the Portuguese territory by the Romans and has been exported for architectural purposes in different continents. PA is a candidate for World Heritage Stone designation, through the Geoscience Department of the University of Coimbra (Portugal). This stone is often subjected to chemical–physical decay and biodeterioration, which was one of the main reasons for its selection.

PA limestone was characterized using the following technological tests: (i) compressive strength, (ii) thermal conductivity, (iii) volume heat capacity, (iv) thermal diffusivity, (v) Leeb D hardness (HLD), and (vi) P wave speed (m/s). All these properties were measured in cubic specimens of 5 × 5 × 5 cm. Specimens of 1.5 × 1.5 × 2.5 cm were employed to measure the real, bulk, and solid density; effective porosity; closed porosity; and immersion coefficient. Vapor permeability specimens had 2.5 × 2.5 cm dimensions with a variable thickness (t), ranging from 3 to 5 mm.

Concerning the inoculation and the following climatic chamber exposition test, 6 specimens with 2 × 2 × 1 cm dimensions were used. Two sets of specimens were used. The first set consisted of 3 inoculated specimens that were subjected to the historical climatic context. A second set of 3 inoculated specimens were subjected to a predicted climatic context. Three non-inoculated control specimens were added to each set.

2.2. Methods

The mineralogical composition of the stone was identified by X-ray diffraction with a Bruker D8 Discover diffractometer (Bruker Company, Karlsruhe city, Germany). The CuKα radiation tube operated at 40 kV and 40 mA. The XRD peaks were measured between 2° and 75° 2θ, with 1 s counting time per point. The Powder Diffraction Database (PDF-ICDD, International Centre for Diffraction Data) using Bruker EVA software (version V7.5.0 32 bit) was used to identify the crystalline phases.

Hardness was measured using a portable tester (Leeb D EQUOTIP, Proceq), with the wireless software platform EQUOTIP LIVE (version 3.1.4). The instrument was indirectly verified, according to the ISO16859-2 standard.

Measurements of the P wave speed (Vp) were carried out using a portable PUNDIT PL200 PROCEQ.

The thermal conductivity coefficient, volume heat capacity, and thermal diffusivity were measured using an ISOMET 2114 thermal effusivity meter.

The point load index (Is_{50}) was determined with a point load tester (Controls D550).

During the water vapor permeability test, the EN 15803:2010 standard was followed [43].

Compressive strength (σ_C) was assessed by uniaxial compression testing in accordance with the EN 1926: 2006 standard on cubic specimens (50 mm side) [44]. The employed instrument was an EL200 hydraulic press produced by PEGASIL (1200 kN capacity). The remaining physical features, such as real, solid, and bulk density, were measured with the help of a Quantachrome ULTRAPY1200e pycnometer.

Rhodotorula sp. was previously isolated near the Mosteiro de Alcobaça (Portugal, 39°32′ N–8°58′ W) from natural stone exposed to an outdoor environment. Following the isolation, the yeast was characterized and sequenced (Table 1, Figure 2) [45]. The access number on GenBanck is CCLBH-F7L3 OR802143.

Table 1. Characterization of the *Rhodotorula* sp. yeast isolate used in this study.

Closest Related Type Strain on Basis of ITS	Family	Class	Phylum
Rhodotorula mucilaginosa	Sporidiobolaceae	Microbotryomycetes	Basidiomycota

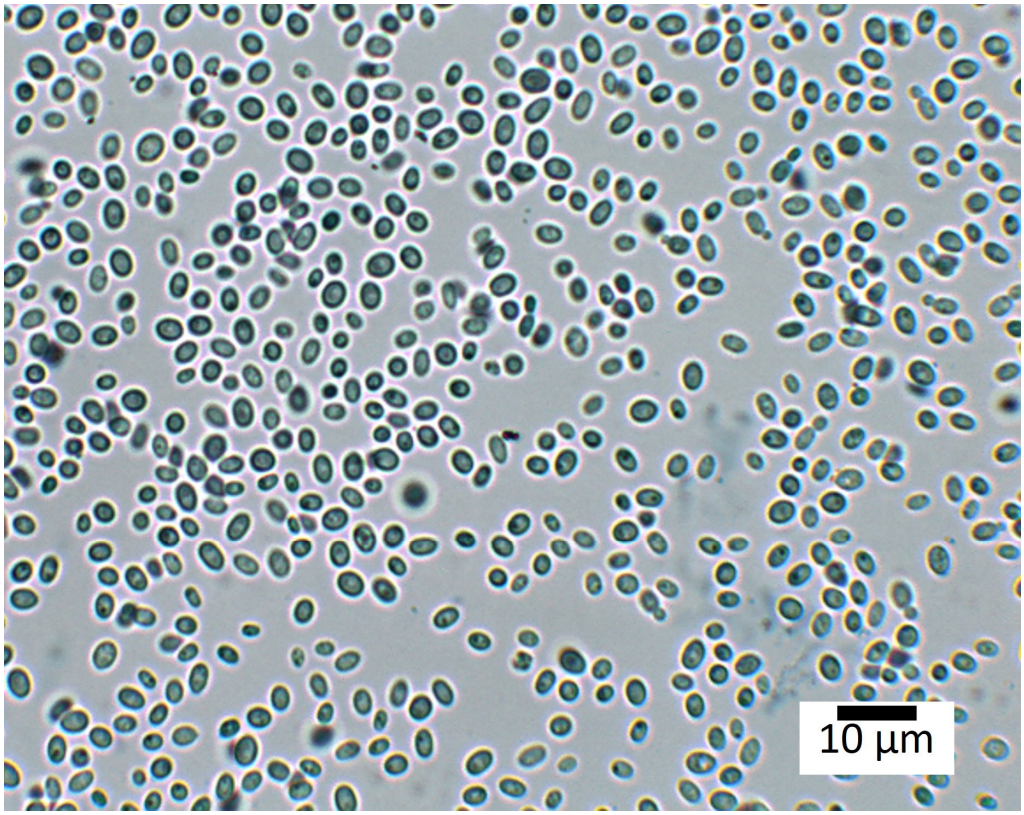

Figure 2. Microscopic features of *Rhodotorula mucilaginosa* (400× magnification).

Fresh cultures were prepared in slants using Yeast Extract Peptone Dextrose (YEPD) culture medium (yeast extract, dextrose, and peptone) and grown for 4 days at 28 °C. The cells were placed in a sterilized physiological saline medium (0.9% w/v). Each limestone mock-up was inoculated with 200 µL of this cell-suspension solution corresponding to 8×10^7 cells.

The first set of limestone specimens was placed for 90 days in an ARALAB FITOCLIMA 600. This was programmed with a fixed temperature of 26.5 °C, 74.9% relative humidity, and an atmospheric CO_2 concentration of about 420 ppm. The data of temperatures represent the annual averages (period 1995–2014) of the Paraiba region (Brazil, coordinates 7°09′ S–36°49′ W), which was selected as a reference and is mainly affected by a humid tropical climate (Figure 3a).

The years between 1995 and 2014 were selected as the historical period because this time span is used as the basis for climatic projections by the Climate Change Knowledge Portal [46].

Regarding the relative humidity, no data were available for the entire Paraiba district. For this reason, the average annual relative humidity of the capital city Joao Pessoa (period 1995–2014) was used. The climatic data of T and rH are available on the INMET website [47]. The atmospheric concentration of CO_2 during the historical period from 1995 to 2014 is regarded as representative of the levels in the year 2023. It was measured using a portable CO_2 EXTECH CO22O.

It is essential to emphasize that despite the observed period of meteorological data spanning from 1995 to 2014, during which the atmospheric CO_2 concentration was about 378 ppm, the climatic chamber, unfortunately, lacked the capability to replicate an environment with a lower CO_2 concentration than the historical ambient level (about 420 ppm). This concentration, in fact, represented the lower limit of the chamber.

Similarly, and in parallel, the second set of limestone specimens was placed for 90 days in another climatic chamber, the ARALAB FITOCLIMA 300 EDTU. This was programmed with a fixed temperature of 30.2 °C, 78.2% relative humidity, and about 1135 ppm of

atmospheric CO_2 to mimic the predicted atmospheric conditions of the SSP5-8.5 scenario in the Paraiba region (period 2080–2099). The projections of temperatures are relative to the Coupled Model Intercomparison Project (CMIP) 6 supporting the IPCC's Sixth Assessment Report [46] (Figure 3a,b).

The predicted CO_2 atmospheric concentration was calculated using the MAGICC7 climate model and selected as about 1135 ppm (max. concentration predicted for the year 2100).

For the average annual relative humidity in the period 2080–2099, the Copernicus software projections [48], referred to the scenario CMIP 6, SSP5-8.5 in Paraiba territory, were used. The climatic model CMCC-ESM2 at level 1000 hPa has been used for the projections.

In both climatic chambers, the internal light followed the natural dark/light cycles with a maximum illuminance of 6 lx. Each mock-up received a weekly addition of 150 µL of Yeast Extract Peptone Dextrose (YEPD) medium culture.

The climatic chamber settings are presented in Table 2.

Table 2. Average annual temperature, relative humidity, and CO_2 atmospheric concentration of historical and foreseen climatic conditions of the Paraiba region (Brazil).

Paraiba Region (Brazil)	Historical Conditions (Period 1995–2014)			Foreseen Conditions, CMIP 6, IPCC SSP5-8.5 Scenario (Period 2080–2099 AD), Figure 3a,b		
	Average Annual Temperature	Average Annual Relative Humidity	CO_2 Atmospheric Concentration	Average Annual Temperature	Average Annual Relative Humidity	CO_2 Atmospheric Concentration (ppm)
	26.5 °C	74.9%	~420 ppm	30.2 °C	78.2%	~1135 ppm

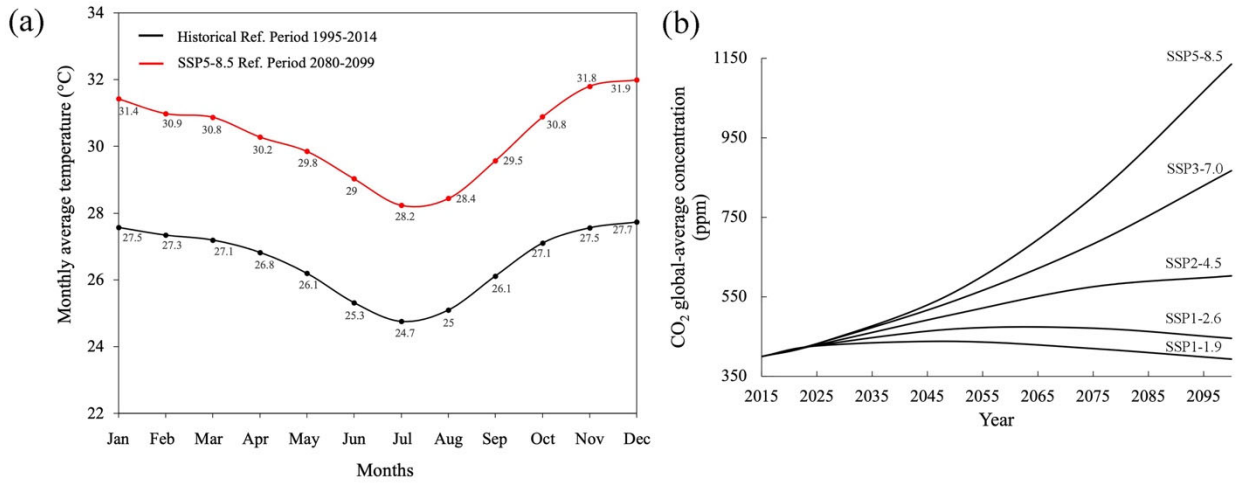

Figure 3. (**a**) Monthly average temperatures according to the historical period (1995–2014) and SSP5-8.5 scenario (2080–2099); (**b**) foreseen atmospheric CO_2 concentrations for different shared socio-economic pathways (SSPs) projected by MAGICC7 climate model.

Three-dimensional models of the specimen surfaces were created using a Hirox-01 Digital Microscope equipped with a Nano Point Scanner (NPS). Each map of a 4 cm^2 surface was developed using 200 scanning lines (scanning speed of 2000 µm/s) and elaborated with the help of MOUNTAINS 7.0 software.

The metabolic activity was determined by the reduction of MTT (3-[4,5-dimethylthiazol-2-yl]-2,5-diphenyltetrazolium bromide) by cell dehydrogenases. The MTT assay is a colorimetric method that allows the determination of active cells based on their capacity to reduce MTT (yellow compound) to formazan (purple compound), with the intensity of the purple color being proportional to the number of viable cells. This protocol has successfully been applied in similar studies [6], giving accurate and reliable data.

At the end of the test, the specimens were removed from the climatic chambers and photographed using the Hirox-01 digital microscope, and 3D surface models were created. Each specimen was then placed in a 50 mL Falcon tube. Then, 3 mL of sterilized physiological saline medium (0.9% w/v) was added, and the cells were extracted from the surface. The MTT assay was performed according to Dias et al. [4]. Each specimen was assessed in duplicate.

3. Results and Discussion

Pedra de Ançã (*PA*) is a micritic limestone and has geological characteristics in common with many lithotypes globally used in architecture. This is the reason it was selected for the assessment of the biodeterioration effect in the present research [49].

This limestone has a mediocre hardness and can be easily degraded by weathering. Its smooth finish can easily deteriorate due to an increase in roughness. This process causes an increase in the surface permeability. At the same time, the greater roughness reduces the rainwater runoff, leaving the surface humid for a long time. Additionally, the effective porosity of *PA* ranges between 18.7 and 22.4% (Table 3). Water absorption for total immersion at atmospheric pressure is sufficiently high, with imbibition coefficients between 8.1% and 12.2%. The vapor permeability range is $1.8 \times 10^{-11} < k_V < 2.1 \times 10^{-11}$ g/m·s·Pa, and the average gas-driven permeability has been evaluated as about 70 mDarcy.

Accordingly, *PA* absorbs large amounts of liquid solutions and allows the vapor to easily permeate the stone. The wettability of the surface, due to the rapid increase in roughness, is a key factor.

The retention of water in the stone, linked to all the above-mentioned physical features, supports the growth of microorganisms.

Biochemically speaking, the stone does not have substantial nutritional properties as it presents a simple mineralogy composed of 99% calcite and 1% quartz.

Table 3. Physical–mechanical features of *PA* limestone.

Physical–Mechanical Feature	Range
Real density (g/cm^3)	$2.72 < \rho_R < 2.73$
Bulk density (g/cm^3)	$2.05 < \rho_B < 2.17$
Effective porosity (%)	$18.7 < \Phi_0 < 22.4$
Closed porosity (%)	$0.54 < \Phi_C < 1.91$
Total immersion coefficient (%)	$8.1 < CI_W < 12.2$
Point load strength index (MPa)	$1.62 < Is_{50} < 2.63$
Compressive strength (MPa)	$21.7 < \sigma_C < 24.4$
Thermal conductivity (W/m·K)	$1.64 < k < 1.78$
Volume heat capacity (J/m^3·K)	$2.04 \times 10^6 < s < 2.11 \times 10^6$
Thermal diffusivity (m^2/s)	$0.78 \times 10^{-6} < \alpha < 0.84 \times 10^{-6}$
Leeb D hardness (HLD)	$547 < L_H < 604$
Vapor permeability (g/m·s·Pa)	$1.8 \times 10^{-11} < k_V < 2.1 \times 10^{-11}$
P wave speed (m/s)	$4850 < V_P < 5102$

As described in the methods section, *PA* limestone was inoculated and placed in two different climatic chambers simulating the meteorological conditions of the historical period (1995–2014) and the predicted period (2080–2099). The evaluation of the physical biodeterioration of the samples was performed using NPS micro-topographic maps. On the left side of Figure 4, topographic maps relative to the sample surfaces at the initial stage (pre-aging) are presented and, on the right, topographic maps of the final stage (post-aging) are shown.

Topographic dissimilarities can be detected in the post-aging maps and are traceable to two types of positive morphologies: (1) When located in the border of the stone specimens, these are mainly due to deposits of microorganisms and, at the same time, residual of the culture medium. (2) When positive morphologies are in the central part of the specimen surface, they can be due to partial swelling. This occurs when the biofilm dries out and detaches from the stone surface. When this process happens, the biofilm removes a

micrometric layer of stone. This type of alteration is well visible in specimens 1 and 3 (post-aging) (Figure 4), with elevations of the positive morphologies ranging from 100 to 400 µm.

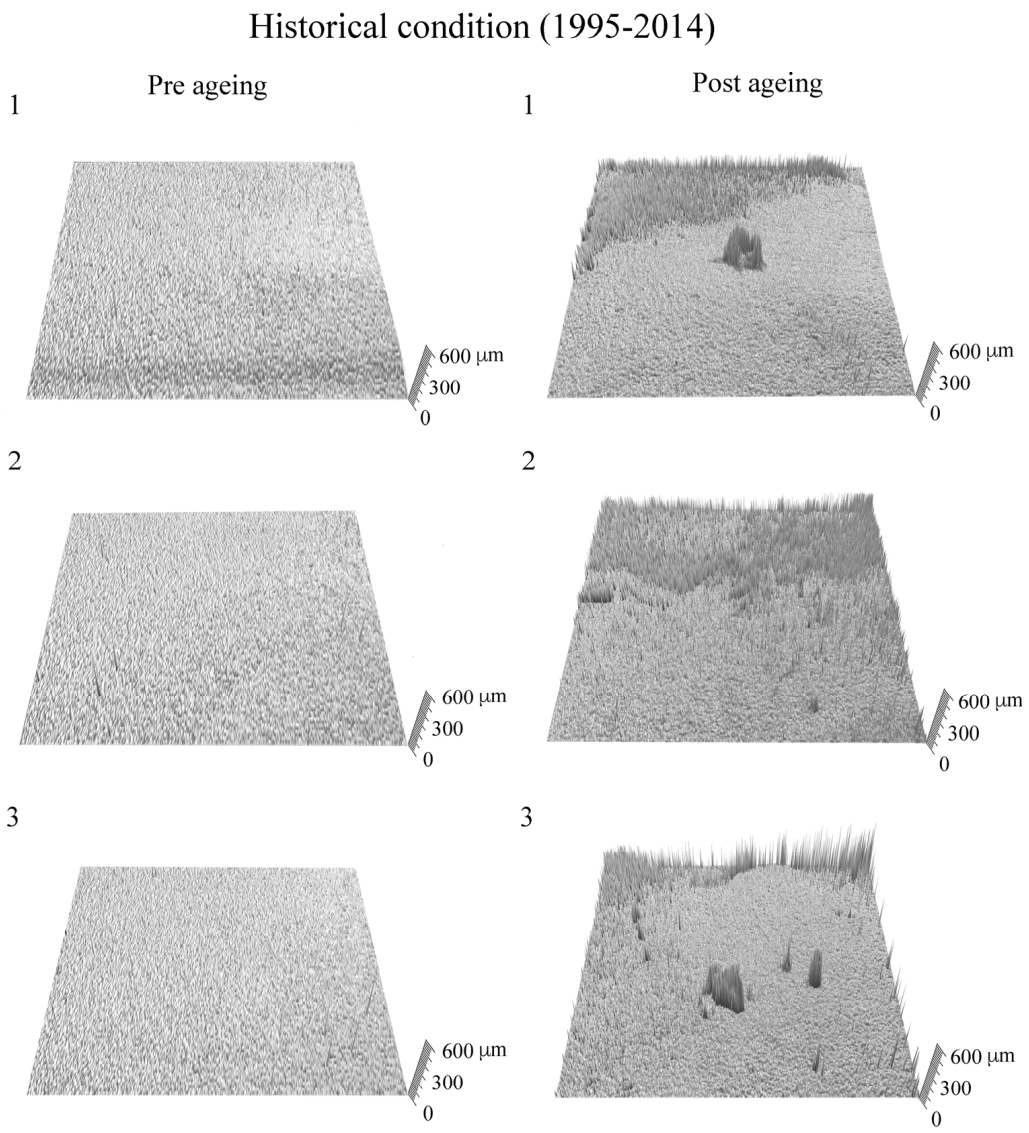

Figure 4. On the left side, micro-topographic maps relative to the sample surfaces at the initial stage (pre-aging); on the right, micro-topographic maps after aging simulating the historical (1995–2014) climatic features of the Paraiba region. Positive morphologies are visible in the peripheral areas due to the thickening of the biofilm and accumulations of residue due to the deposition of the culture liquid.

The swelling phenomenon also occurs, although to a lesser extent, in samples exposed to the SSP5-8.5 scenario (Figure 5). In this circumstance, positive morphologies are visible in the peripheral areas due to the thickening of the biofilm and accumulations of residue due to the deposition of the culture liquid. The residues are visible in Figure 6, where the RGB photos of the specimen surfaces in the post-aging phase are shown.

The results of the determination of metabolic activity by the reduction of MTT (Figure 7) indicate that the growth of the selected strain *Rhodotorula* sp. was influenced by the different environmental conditions. This variation should be mainly related to the different levels of CO_2. This is because the optimal growth temperature of this mesophilic strain is generally considered to be between ~25 °C and ~30 °C (as in the historical and predicted conditions). In addition, the reproduced relative humidities in both conditions are very similar (74.9% vs. 78.2%). Thus, it was observed that the specimens subjected to

aging under a lower amount of CO_2 showed a greater proliferation capacity of this specific microorganism on the *PA* limestone substrate. Due to the similarity of T and rH between historical and foreseen climates and the great CO_2 difference, it is expected that microbial growth will be mainly affected by this factor.

Rhodotorula species, like many yeasts, are known for their CO_2 tolerance and adaptability to various environmental conditions [50]. However, while they can adapt to a wide range of temperatures and relative humidity, extremely high CO_2 concentrations may induce stress in the cells, leading to atypical physiological responses and, consequently, a decreased growth rate.

The genus *Rhodotorula* is made up of yeasts that are considered facultative aerobes. However, their preference for aerobic environments may be due to their sensitivity to carbon dioxide (CO_2). High concentrations of CO_2 can be inhibitory to the growth of some yeasts, including *Rhodotorula*, since carbon dioxide can acidify the environment, inhibiting the growth of microbes. Additionally, CO_2 can affect the pH of the culture medium, making it more acidic. Yeast typically thrives in environments with neutral or slightly alkaline pH [51].

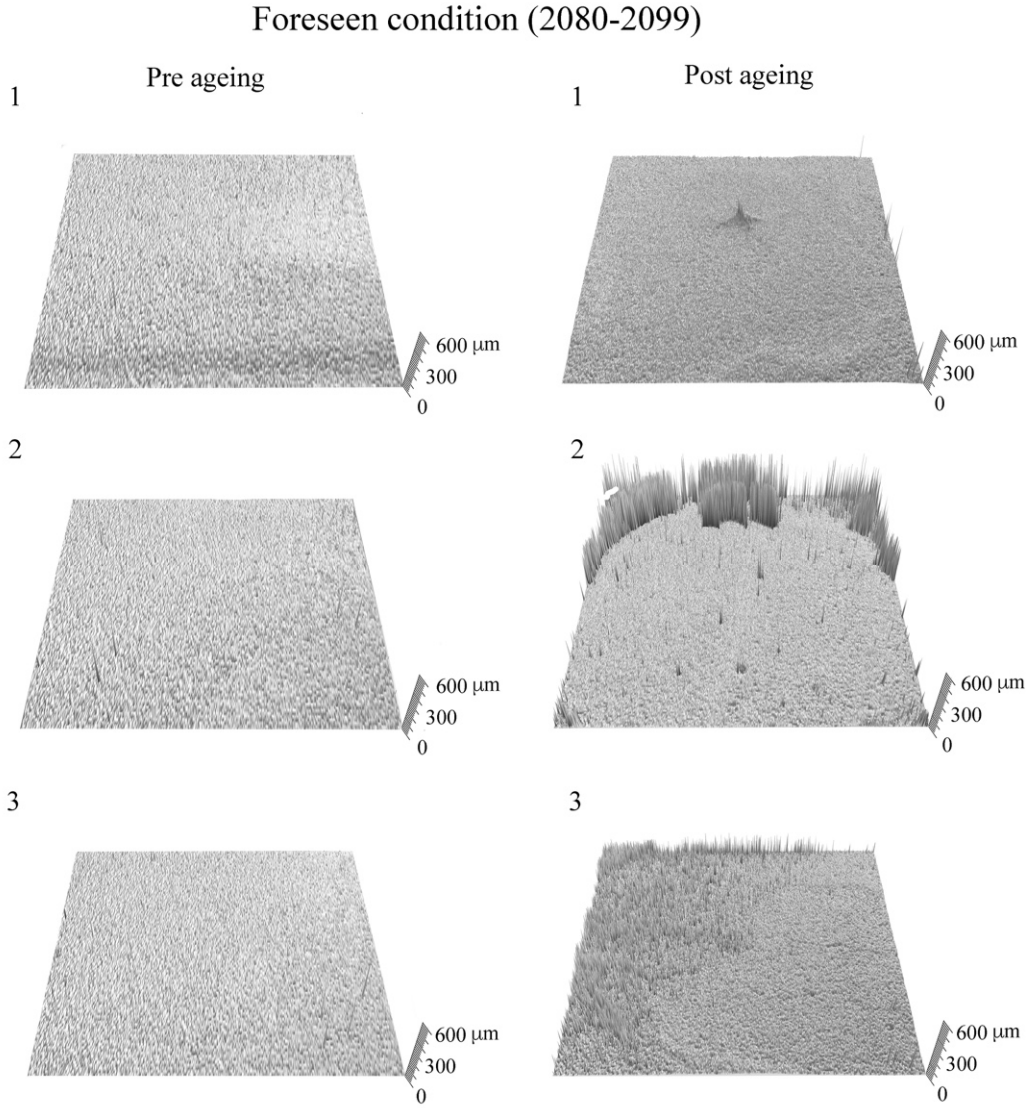

Figure 5. On the left, micro-topographic maps relative to the sample surfaces before aging; on the right, micro-topographic maps after aging simulating the predicted (2080–2099) climatic features of the Paraiba region. Positive morphologies (biofilm) are visible, even if they are less evident with respect to the historical climatic conditions.

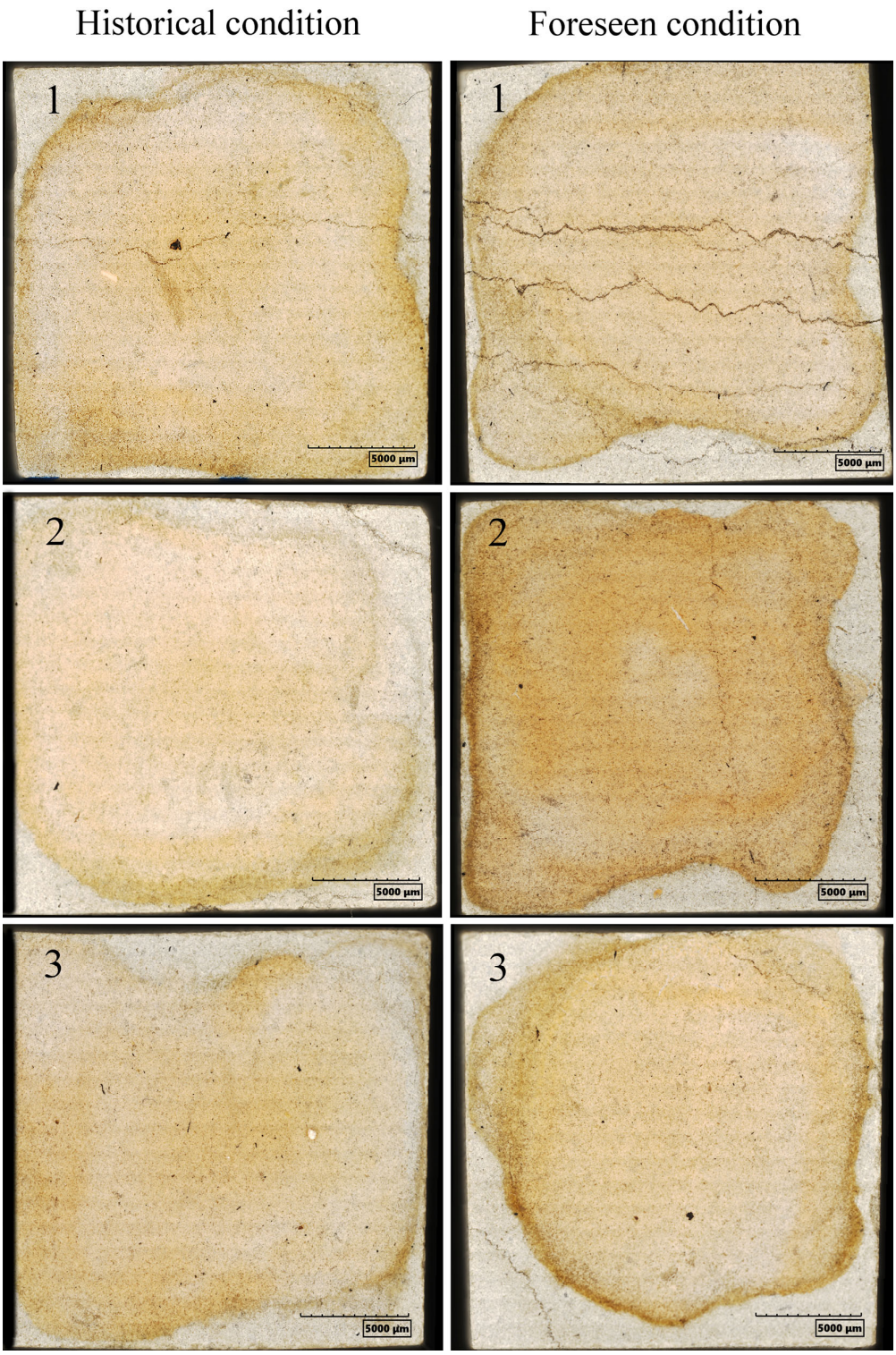

Figure 6. RGB photographs of the limestone mock-up surfaces in the post-aging stage. The residue of biofilm and residue of liquid culture with orange color are well documented.

However, it is important to bear in mind that the tolerance of *Rhodotorula* to CO_2 can vary between different species or strains. In addition, the growth environment and the composition of the culture medium can influence *Rhodotorula's* response to CO_2. Therefore, the exact reasons may vary and require more studies to be fully understood.

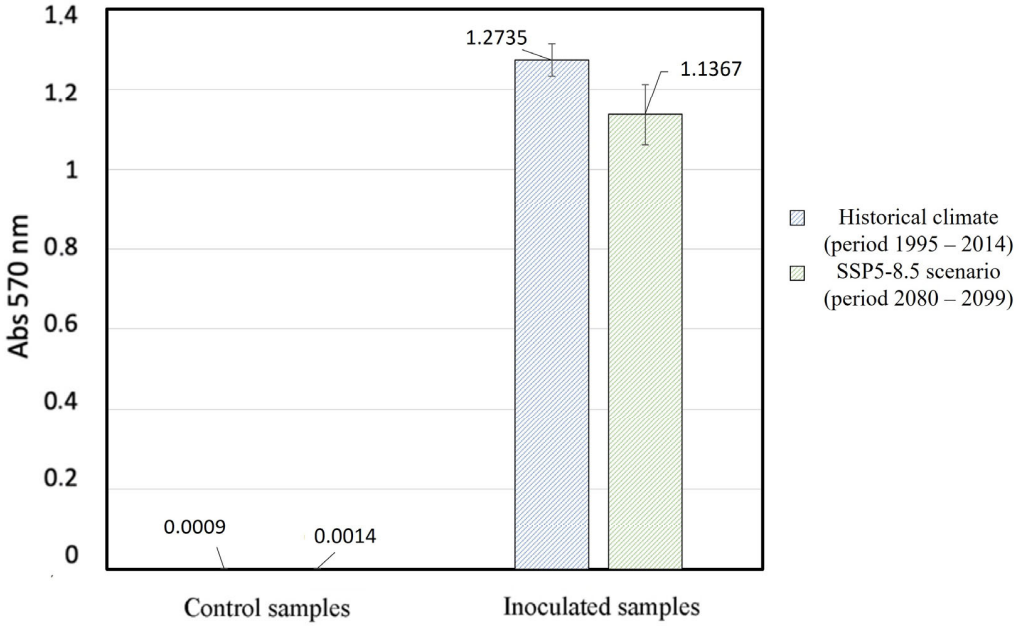

Figure 7. Determination of cell viability in the specimens under study, through spectrophotometric reading of the solutions at 570 nm (n = 6 measurements).

4. Conclusions

This study demonstrates the adaptation capacities of the *Rhodotorula* sp. biodeteriogen in the historical and predicted climatic contexts of humid tropical climates. The material tested as a substrate is *Pedra de Ançã* (*PA*), a candidate for World Heritage Stone. It is a micritic limestone with petro-physical and mineralogical features predisposing it to biodeterioration. This pathology was mainly detected on the specimen set exposed to the historical climatic conditions (i.e., T = 26.5 °C, rH = 74.9%, atmospheric CO_2 ~ 420 ppm). The set of specimens subjected to future climatic conditions (i.e., T = 30.2 °C, rH = 78.2%, atmospheric CO_2 ~ 1135 ppm) depicted less evident biofilm formation. Positive morphologies on the specimen surface can be due to a partial swelling of the biofilm. This occurs when it dries out and detaches from the surface of the stone, removing a micrometric layer of material.

The analysis of the cell viability for the two sets demonstrates how, for the same limestone substrate, *Rhodotorula* sp. has a better growth capacity in conditions of historical CO_2 atmospheric concentrations, temperature, and humidity. The key factor in this variance is probably linked to the amount of future atmospheric CO_2, which, compared to the historical one, undergoes an increase of ~715 ppm. Differently, small increases in temperature and humidity would be irrelevant in conditioning the dynamics of biodecay. The crucial processes of rain acidification, humidity, and moisture due to the increase in atmospheric CO_2 concentration could adversely affect the micro-environment of the stone substrate, the biochemical functions of the microorganisms, and the acidity of the culture media. As a result, the microbial activity of *Rhodotorula* sp. could be limited, and consequently, the cell viability could be reduced.

The acquired information, therefore, demonstrates that based on the SSP5-8.5 scenario (period 2080–2099), in humid tropical environments, the biodegradation dynamics due to *Rhodotorula* would slow down on micritic limestones. Aesthetically, we would expect to see biofilms characterized by a pinkish color less intense than that seen historically due to a minor microbial density and consequently less production of carotenes.

Future studies should be carried out by involving and mixing different groups of microorganisms, different climatic scenarios, and different substrates.

Author Contributions: Conceptualization, F.S. and L.D.; methodology, F.S., L.D. and C.L.; software, F.S., L.D., C.L. and A.T.C.; validation, F.S., V.P., C.L., J.M., L.D. and A.T.C.; formal analysis, F.S., V.P., C.L. and L.D.; investigation, F.S. and L.D.; resources, J.M. and A.T.C.; data curation, F.S., V.P., C.L. and L.D.; writing—original draft preparation, F.S.; writing—review and editing F.S., V.P., C.L., L.D., A.T.C. and J.M.; visualization, F.S., J.M. and A.T.C. supervision, F.S.; project administration, F.S.; funding acquisition, J.M. and A.T.C. All authors have read and agreed to the published version of the manuscript.

Funding: This research was funded by INOVSTONE4.0 (POCI-01-0247-FEDER-024535), co-financed by the European Union through the European Regional Development Fund (FEDER) and Fundação para a Ciência e Tecnologia (FCT) under the project UID/Multi/04449/2013 (POCI-01-0145- FEDER-007649), and Fundacao para a Ciencia e Tecnologia (FCT) under the project UIDB/04449/2020 and UIDP/04449/2020. The authors gratefully acknowledge the European Communion—Portugal, Grant Contract Number: Sustainable Stone by Portugal Call: 2021-C05i0101-02—agendas/alianças mobilizadoras para a reindustrialização—PRR, Proposal: C632482988-00467016. Fabio Sitzia gratefully acknowledge the Recursos Humanos Altamente Qualificados (RHAQ), University of Evora, funding number: ALT20-05-3559-FSE-000074.

Data Availability Statement: Data are contained within the article.

Conflicts of Interest: The authors declare no conflict of interest.

References

1. Pires, V.; Amaral, P.M.; Simão, J.A.R.; Galhano, C. Experimental Procedure for Studying the Degradation and Alteration of Limestone Slabs Applied on Exterior Cladding. *Environ. Earth Sci.* **2022**, *81*, 59. [CrossRef]
2. Sitzia, F. Climate Change and Cultural Heritage: From Small- to Large-Scale Effects—The Case Study of Nora (Sardinia, Italy). *Heritage* **2022**, *5*, 3495–3514. [CrossRef]
3. Sitzia, F.; Lisci, C.; Pires, V.; Alves, T.; Mirão, J. Laboratorial Simulation for Assessing the Performance of Slates as Construction Materials in Cold Climates. *Appl. Sci.* **2023**, *13*, 2761. [CrossRef]
4. Dias, L.; Pires, V.; Sitzia, F.; Lisci, C.; Candeias, A.; Caldeira, A.T.; Mirão, J. Evaluating the Biosusceptibility of Natural Stone as an Supporting Tool to Prevent Cultural Heritage Biodeterioration. *Eur. Phys. J. Plus* **2023**, *138*, 570. [CrossRef]
5. Addesso, R.; Baldantoni, D.; Cubero, B.; De La Rosa, J.M.; González Pérez, J.A.; Tiago, I.; Caldeira, A.T.; De Waele, J.; Miller, A.Z. A Multidisciplinary Approach to the Comparison of Three Contrasting Treatments on Both Lampenflora Community and Underlying Rock Surface. *Biofouling* **2023**, *39*, 204–217. [CrossRef] [PubMed]
6. Prieto, B.; Vázquez-Nion, D.; Fuentes, E.; Durán-Román, A.G. Response of Subaerial Biofilms Growing on Stone-Built Cultural Heritage to Changing Water Regime and CO_2 Conditions. *Int. Biodeterior. Biodegrad.* **2020**, *148*, 104882. [CrossRef]
7. Schimel, D.S. Terrestrial Ecosystems and the Carbon Cycle. *Glob. Change Biol.* **1995**, *1*, 77–91. [CrossRef]
8. Korner, C. Biosphere Responses to CO_2 Enrichment. *Ecol. Appl.* **2000**, *10*, 1590–1619. [CrossRef]
9. DeLucia, E.H.; Hamilton, J.G.; Naidu, S.L.; Thomas, R.B.; Andrews, J.A.; Finzi, A.; Lavine, M.; Matamala, R.; Mohan, J.E.; Hendrey, G.R.; et al. Net Primary Production of a Forest Ecosystem with Experimental CO_2 Enrichment. *Science* **1999**, *284*, 1177–1179. [CrossRef]
10. Querijero-Palacpac, N.M.; Martinez, M.R.; Boussiba, S. Mass Cultivation of the Nitrogen-Fixing Cyanobacterium Gloeotrichia Natans, Indigenous to Rice-Fields. *J. Appl. Phycol.* **1990**, *2*, 319–325. [CrossRef]
11. Huertas, E.; Montero, O.; Lubián, L.M. Effects of Dissolved Inorganic Carbon Availability on Growth, Nutrient Uptake and Chlorophyll Fluorescence of Two Species of Marine Microalgae. *Aquac. Eng.* **2000**, *22*, 181–197. [CrossRef]
12. Oren, R.; Ellsworth, D.S.; Johnsen, K.H.; Phillips, N.; Ewers, B.E.; Maier, C.; Schäfer, K.V.R.; McCarthy, H.; Hendrey, G.; McNulty, S.G.; et al. Soil Fertility Limits Carbon Sequestration by Forest Ecosystems in a CO_2-Enriched Atmosphere. *Nature* **2001**, *411*, 469–472. [CrossRef]
13. Morales, E.; Rodríguez, M.; García, D.; Loreto, C.; Marco, E. Crecimeinto, Producción de Pigmentos y Exopolisacáridos de La Cianobacteria Anabaena Sp. PCC 7120 En Función Del PH y CO_2. *Interciencia* **2002**, *27*, 373–378.
14. Singh, S.P.; Singh, P. Effect of CO_2 Concentration on Algal Growth: A Review. *Renew. Sustain. Energy Rev.* **2014**, *38*, 172–179. [CrossRef]
15. Li, W.; Xu, X.; Fujibayashi, M.; Niu, Q.; Tanaka, N.; Nishimura, O. Response of Microalgae to Elevated CO_2 and Temperature: Impact of Climate Change on Freshwater Ecosystems. *Environ. Sci. Pollut. Res.* **2016**, *23*, 19847–19860. [CrossRef]
16. Palmqvist, K. Carbon Economy in Lichens. *New Phytol.* **2000**, *148*, 11–36. [CrossRef]
17. Collins, S.; Bell, G. Evolution of Natural Algal Populations at Elevated CO_2. *Ecol. Lett.* **2006**, *9*, 129–135. [CrossRef] [PubMed]
18. Viles, H.A.; Cutler, N.A. Global Environmental Change and the Biology of Heritage Structures. *Glob. Change Biol.* **2012**, *18*, 2406–2418. [CrossRef]
19. Meinshausen, M.; Nicholls, Z.R.J.; Lewis, J.; Gidden, M.J.; Vogel, E.; Freund, M.; Beyerle, U.; Gessner, C.; Nauels, A.; Bauer, N.; et al. The Shared Socio-Economic Pathway (SSP) Greenhouse Gas Concentrations and Their Extensions to 2500. *Geosci. Model Dev.* **2020**, *13*, 3571–3605. [CrossRef]

20. Nuhoglu, Y.; Oguz, E.; Uslu, H.; Ozbek, A.; Ipekoglu, B.; Ocak, I.; Hasenekoglu, I. The Accelerating Effects of the Microorganisms on Biodeterioration of Stone Monuments under Air Pollution and Continental-Cold Climatic Conditions in Erzurum, Turkey. *Sci. Total Environ.* **2006**, *364*, 272–283. [CrossRef] [PubMed]
21. Saiz-Jimenez, C. Deposition of Anthropogenic Compounds on Monuments and Their Effect on Airborne Microorganisms. *Aerobiologia* **1995**, *11*, 161–175. [CrossRef]
22. Del Monte, M. Il Biodegrado Dei Monumenti in Pietra: I Licheni e i "Segni El Tempo". *Il Geologo dell'Emilia Romagna* **2007**, *VII*, 11–55.
23. Bonazza, A.; Messina, P.; Sabbioni, C.; Grossi, C.M.; Brimblecombe, P. Mapping the Impact of Climate Change on Surface Recession of Carbonate Buildings in Europe. *Sci. Total Environ.* **2009**, *407*, 2039–2050. [CrossRef]
24. Gómez-Bolea, A.; Llop, E.; Ariño, X.; Saiz-Jimenez, C.; Bonazza, A.; Messina, P.; Sabbioni, C. Mapping the Impact of Climate Change on Biomass Accumulation on Stone. *J. Cult. Herit.* **2012**, *13*, 254–258. [CrossRef]
25. Cutler, N.A.; Oliver, A.E.; Viles, H.A.; Ahmad, S.; Whiteley, A.S. The Characterisation of Eukaryotic Microbial Communities Onsandstone Buildings in Belfast, UK, Using TRFLP and 454 Pyrosequencing. *Int. Biodeterior. Biodegrad.* **2013**, *82*, 124–133. [CrossRef]
26. Miller, A.Z.; Rogerio-Candelera, M.A.; Dionísio, A.; Macedo, M.F.; Saiz-Jiménez, C. Evaluación de La Influencia de La Rugosidad Superficial Sobre La Colonización Epilítica de Calizas Mediante Técnicas Sin Contacto. *Mater. Constr.* **2012**, *62*, 411–424. [CrossRef]
27. Miller, A.Z.; Dionísio, A.; Laiz, L.; Macedo, M.F.; Saiz-Jimenez, C. The Influence of Inherent Properties of Building Limestones on Their Bioreceptivity to Phototrophic Microorganisms. *Ann. Microbiol.* **2009**, *59*, 705–713. [CrossRef]
28. Prieto, B.; Silva, B. Estimation of the Potential Bioreceptivity of Granitic Rocks from Their Intrinsic Properties. *Int. Biodeterior. Biodegrad.* **2005**, *56*, 206–215. [CrossRef]
29. Cennamo, P.; Caputo, P.; Marzano, C.; Miller, A.Z.; Saiz-Jimenez, C.; Moretti, A. Diversity of Phototrophic Components in Biofilms from Piperno Historical Stoneworks. *Plant Biosyst. Int. J. Deal. All Asp. Plant Biol.* **2016**, *150*, 720–729. [CrossRef]
30. Miller, A.Z.; Sanmartín, P.; Pereira-Pardo, L.; Dionísio, A.; Saiz-Jimenez, C.; Macedo, M.F.; Prieto, B. Bioreceptivity of Building Stones: A Review. *Sci. Total Environ.* **2012**, *426*, 1–12. [CrossRef] [PubMed]
31. Pitzurra, L.; Moroni, B.; Nocentini, A.; Sbaraglia, G.; Poli, G.; Bistoni, F. Microbial Growth and Air Pollution in Carbonate Rock Weathering. *Int. Biodeterior. Biodegrad.* **2003**, *52*, 63–68. [CrossRef]
32. Rosado, T.; Reis, A.; Mirão, J.; Candeias, A.; Vandenabeele, P.; Caldeira, A.T. Pink! Why Not? On the Unusual Colour of Évora Cathedral. *Int. Biodeterior. Biodegrad.* **2014**, *94*, 121–127. [CrossRef]
33. Durgenova, A.; Piksayakina, A.; Bogatov, V.; Salman, A.L.; Erofeev, V. The Economic Damage from Biodeterioration in Building Sector. *IOP Conf. Ser. Mater. Sci. Eng.* **2019**, *698*, 077020. [CrossRef]
34. Dias, L.; Rosado, T.; Battacharia, S.; Candeias, A.; Teresa Caldeira, A.; Mirão, J. Assessing Aesthetic and Structural Deterioration in Historic Buildings. In Proceedings of the 9th Euro-American Congress on Construction Pathology, Rehabilitation Technology and Heritage Management, Granada, Spain, 13–16 September 2022; pp. 596–605.
35. Gaylarde, C.C.; Baptista-Neto, J.A. Microbiologically Induced Aesthetic and Structural Changes to Dimension Stone. *npj Mater. Degrad.* **2021**, *5*, 33. [CrossRef]
36. Moliné, M.; Libkind, D.; Van Broock, M. Production of Torularhodin, Torulene, and β-Carotene by Rhodotorula Yeasts. *Methods Mol. Biol.* **2012**, *898*, 275–283. [CrossRef]
37. Bartoli, F.; Ellwood, N.T.W.; Bruno, L.; Ceschin, S.; Rugnini, L.; Caneva, G. Ecological and Taxonomic Characterisation of Trentepohlia Umbrina (Kützing) Bornet Growing on Stone Surfaces in Lazio (Italy). *Ann. Microbiol.* **2019**, *69*, 1059–1070. [CrossRef]
38. Ekendahl, S.; O'Neill, A.H.; Thomsson, E.; Pedersen, K. Characterisation of Yeasts Isolated from Deep Igneous Rock Aquifers of the Fennoscandian Shield. *Microb. Ecol.* **2003**, *46*, 416–428. [CrossRef]
39. Geiger, R. Classificação Climática de Köppen-Geiger. *Creat. Commons Attrib. Alike 3.0 Unported* **1936**. Available online: https://creativecommons.org/licenses/by-sa/3.0/ (accessed on 20 October 2023).
40. Ribeiro, F. Pedra de Ançã: Contribuição Para a Classificação "Global Heritage Stone Resource". Master's Thesis, University of Coimbra, Coimbra, Portugal, 2017.
41. Columbu, S.; Palomba, M.; Sitzia, F.; Carcangiu, G.; Meloni, P. Pyroclastic Stones as Building Materials in Medieval Romanesque Architecture of Sardinia (Italy): Chemical-Physical Features of Rocks and Associated Alterations. *Int. J. Archit. Herit.* **2020**, *16*, 49–66. [CrossRef]
42. Ferreira, M.; Lidia, G.; Delgado Rodrigues, J. The Ançã Limestones, Coimbra, Portugal. In Proceedings of the EGU General Assembly 2016, Wien, Austria, 17–22 April 2016.
43. *EN 15803:2010*; Conservation of Cultural Property-Test Methods-Determination of Water Vapour Permeability (Δp). Comité Européen de Normalisation: Bruxelles, Belgium, 2010.
44. *EN 1926:2006*; Natural Stone Test Methods-Determination of Uniaxial Compressive Strength. Comité Européen de Normalisation: Bruxelles, Belgium, 2006.
45. Dias, L. STONECOLOR: Color of Commercial Marbles and Limestone–Causes and Changes. Ph.D. Thesis, University of Evora, Évora, Portugal, 2021.
46. Climate Change Knowledge Portal CCKP. Available online: https://climateknowledgeportal.worldbank.org (accessed on 20 October 2023).
47. Instituto Nacional de Meteorologia INMET. Available online: https://portal.inmet.gov.br (accessed on 20 October 2023).
48. European Union's Earth Observation Programme—Copernicus. Available online: https://www.copernicus.eu/en (accessed on 20 October 2023).

49. Fratini, F.; Rescic, S.; Tiano, P. A New Portable System for Determining the State of Conservation of Monumental Stones. *Mater. Struct. Constr.* **2006**, *39*, 139–147. [CrossRef]
50. Wang, S.; Zheng, G.; Zhou, L. Heterotrophic Microorganism Rhodotorula Mucilaginosa R30 Improves Tannery Sludge Bioleaching through Elevating Dissolved CO_2 and Extracellular Polymeric Substances Levels in Bioleach Solution as Well as Scavenging Toxic DOM to Acidithiobacillus Species. *Water Res.* **2010**, *44*, 5423–5431. [CrossRef] [PubMed]
51. Urano, N.; Shirao, A.; Naito, Y.; Okai, M.; Ishida, M.; Takashio, M. Molecular Phylogeny and Phenotypic Characterization of Yeasts with a Broad Range of PH Tolerance Isolated from Natural Aquatic Environments. *Adv. Microbiol.* **2019**, *9*, 56. [CrossRef]